Acoustic Pitfalls of Impedance Tube Measurements

Thomas Graf
Lucerne University of Applied Sciences, Technikumstrasse 21, 6048 Horw, Lucerne, Switzerland
thomas.graf@hslu.ch

Abstract: The sound intensity loss of a hard plate in an impedance tube is investigated. A small air gap is left between the sample edge and the tube wall. The narrow gap causes thermoviscous damping. We show by experiments and numerical simulations that a small air gap produces an absorption peak at low frequencies. The sample in the tube behaves like a microperforated slit-absorber. Based on the numerical simulations a spreadsheet model of slit-absorber panels could be developed. Input parameters to the model are the width of the air gap, the thickness of the panel, the porosity of the panel and the depth of the adjacent air cavity.

Keywords: Acoustic impedance tube, thermoviscous acoustics, finite element modeling (FEM), compact model of microperforated slit-absorber.

1. Introduction

Modern architecture prefers exposed concrete and glass. This leads to rooms with many sound-reflecting surfaces. In order to reduce reverberation to a tolerable level, some hard wall surfaces must be lined with absorber elements. The absorber material is characterized by the absorption coefficient as a function of frequency. This so-called absorption curve can be determined in a reverberation chamber described in the standards SN EN ISO 354 and SN EN ISO 11654. The simpler and more cost-effective method is to measure the absorption in an impedance tube according to the standard SN EN ISO 10534-1 & 2. In the impedance tube only the vertical sound incidence is considered. Nevertheless, it is possible to convert the results of the impedance tube into diffuse sound incidence and thus anticipate the measurement in the reverberation chamber. The conversion takes place by integration over the solid angle 2π, respectively by averaging the incident sound intensity over the half space utilizing Lambert's law. The final result can be found, for example, in the Ref. [1].

The prerequisite for the correct conversion is of course an accurate measurement of the absorption coefficient in the impedance tube. For this the sample must fit perfectly into the cross section of the tube. In practice, the precise fitting often leaves a minimal gap between the sample and the wall of the tube. To understand the effect of the air gap on the absorption characteristics of the material, we performed experiments with the impedance tube and numerical calculations by the method of finite elements (FEM).

In section 2. we describe the measuring principles of the impedance tube. Section 3. describes the simulation set-up. The extraction of the absorption coefficient, or better the loss factor β from the numerical calculations is explained in section 4. The results are discussed in section 5. A compact model that emulates the experimental and numerical absorption curves is presented in section 6. The final section 7. summarizes our findings.

2. Experimental Setup

The experiments were performed in an impedance tube developed by the Fraunhofer Institute (Fig. 1.). The software for the analysis was written by Müller BBM (m|abstube 1.6, Müller-BBM GmbH 2015).

The experiment determines the absorption coefficient of a sample as follows. A loudspeaker at the top of the vertical tube generates a frequency sweep. The acoustic pressure in the tube is measured as a function of frequency by an array of four microphones. The microphones are positioned at three different heights x_1, x_2 and x_3 above the sample. That signifies that one frequency sweep is performed for each height. The complex pressure reflection coefficient r is then determined by the method of wave separation (see below). The absorption coefficient α, or better the loss factor β is defined as:

$$\beta = 1 - |r|^2 \quad (1)$$

The tube used for this study has a front opening and a square cross section of $200 \times 200\ \text{mm}^2$ (Fig. 1.). This makes it easy to position the sample and to cut and adjust the sample to size. To validate the computations we prepared a sound-hard MDF-board of 19 mm thickness. The board has 199 mm edge length, thus leaving a gap of 0.5 mm between sample and tube wall, see figure 2.a. Plots of the absorption coefficient versus frequency presented below demonstrate that the sample in the tube behaves as a slit-absorber. The sample was then sealed with plasticine at all four edges (Fig. 2.b). Measurements showed that the air-tight sample now behaves sound-hard and almost no absorption can be detected.

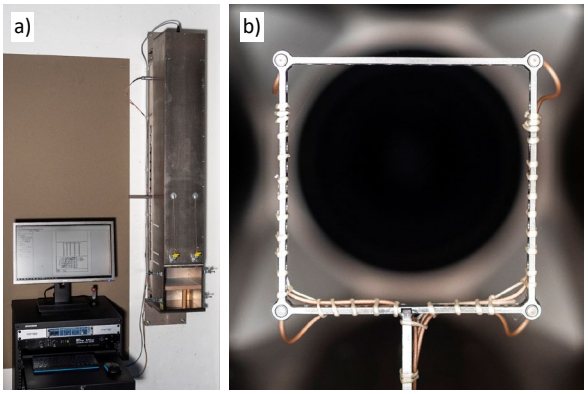

Figure 1. a) Impedance tube of square cross-section and front opening. The sample can be placed at a maximum of 25 cm above the sound-hard bottom termination. **b)** An array of four microphones is visible inside the tube allowing for measurements in a wide range of frequencies. The circular loudspeaker can be seen in the background, surrounded by four sound absorbing elements in the corners of the tube.

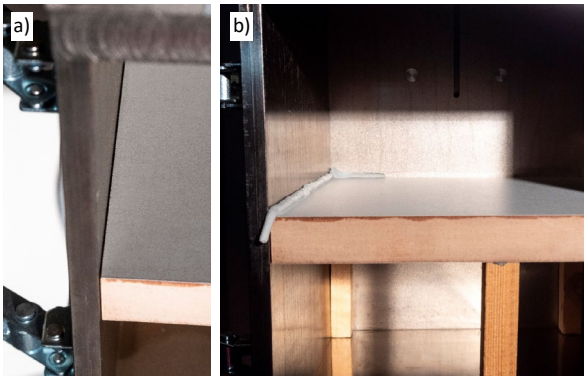

Figure 2. a) Sample inserted into the impedance tube. A gap of approximately 0.5 mm width can be detected between the sample and the tube wall. **b)** The gap is sealed with plasticine. For reliable panel absorption measurements, the sample must be sealed and firmly attached to the supports

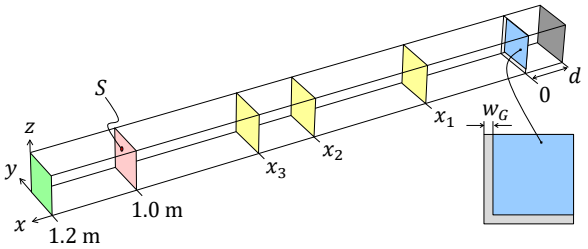

Figure 3. Sketch of the domain geometry for the simulation. Due to symmetry only a quarter tube needs to be calculated. The position of the sample is shown as the blue plane at $x = 0$. The enlargement of that plane displays the gap of width w_G between the sample and the wall of the tube. Red is the source plane at $x = 1.0$ m. The green and the grey plane are the absorbing and the reflecting termination of the tube, respectively. The three yellow planes at x_1, x_2 and x_3 are used to determine the loss factor of the sample plus gap, see text. The geometry for the simulation is identical to that of the experimental tube. In particular the distance $d = 0.1$ m corresponds to the height of the wooden supports in Fig. 2b.

3. Numerical Setup

The numerical results were generated with the program COMSOL Multiphysics ® [2]. The *Pressure Acoustics* module in the *Frequency Domain* interface was employed. The program solves the Helmholtz equation for the pressure field in the fluid domain by the method of finite elements (FEM). The *Narrow Region* domain as well as the *Thermoviscous Acoustics* domain were used for the slit region between the sample and the wall of the impedance tube. Models of the narrow region acoustics are discussed in Ref. [3]. The theory of thermoviscous modeling can be studied in Ref. [4] and references therein. Figure 3 displays the geometry of the simulation domain. The impedance tube is oriented along the x-axis. The sample is placed at the position $x = 0$. There exists a gap w_G between the sample and the wall of the tube. The source is 1.0 m away from the sample plane. The source was either an *Interior Normal Velocity* or a *Monopole Point Source* at the position S in the sketch of Fig. 3. The highest frequencies computed are far below the first cutoff frequency of the tube at 850 Hz. Both source types excited only acoustic plane waves in the tube. At $x = 1.2$ m the tube is terminated with a matched impedance and no sound reflections occur. The impedance at the opposite termination corresponds to a wall reflection coefficient of $r = 0.999$.

The domain mesh was *Free Triangular*. In the narrow region of the slit a swept mesh was employed (see Fig. 4.). The thickness of the thermoviscous layer is $\delta_{visc} = 0.22[\text{mm}]\sqrt{\frac{100[\text{Hz}]}{f}}$, where f is the frequency of the sound wave, see Ref. [5]. The maximum frequency analyzed was 500 Hz corresponding to $\delta_{visc}(500\ \text{Hz}) \cong 0.1$ mm. At frequencies close to 500 Hz the computations were performed with layer elements slightly thicker than the thickness recommended in Ref. [5] for the viscous boundary layer. Nevertheless, velocity plots (figures 5. and 6.) and comparison to *Narrow Region* calculations demonstrated the validity of the utilized element size.

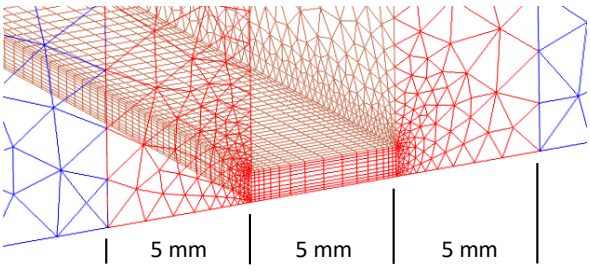

Figure 4. Mesh in the slit region. The red wireframe corresponds to the mesh edges in the *Thermoviscous Acoustics* domain. The mesh for the *Pressure Acoustics* module is represented by the blue wireframe. The slit is 0.5 mm wide and 5 mm deep (along x-axis in Fig. 3.).

4. Analyses of the Computations

To emulate the experiments acoustic plane waves were excited from the source position S (see Fig. 3.) at various frequencies between 10 and 500 Hz. At locations x_1, x_2 and x_3 (Fig. 3.) the acoustic pressure was averaged (*aveop*) over the cross-section of the impedance tube yielding three complex valued pressures p_1, p_2 and p_3. Employing the method of wave separation and using the relation (see e.g. Ref. [6])

$$r_{12} = -e^{-i2kx_1}\frac{1-\frac{p_1}{p_2}e^{-ik\Delta x_{12}}}{1-\frac{p_1}{p_2}e^{ik\Delta x_{12}}} \quad (2)$$

among pairs of the acoustic pressure e.g. p_1 and p_2 separated by $\Delta x_{12} = x_2 - x_1$ the complex reflection coefficient r can be calculated for different combinations: r_{12}, r_{13} and r_{23}. The parameter k in the expression is the wave number which relates to the frequency f and the speed of sound c via $2\pi f = kc$. The three reflection coefficients are averaged to yield $r = (r_{12} + r_{13} + r_{23})/3$. Note that the three values r_{12}, r_{13} and r_{23} should theoretically be equal. The intensity loss factor is finally calculated according to Eq. (1).

Instead of using the technique of wave separation and Eq. (2) it is possible to determine the pressure reflection coefficient r by the minimum-maximum procedure, see e.g. Refs. [6] and [7]. At low frequency, i.e. at large wavelength it is often not possible to detect the minimum nor the maximum of the absolute pressure value in a short tube domain. In this case, the min-max method is not applicable.

Yet another and straightforward procedure to determine r is utilizing the *Port* formulation recently implemented in the COMSOL acoustics module, see for example Ref. [8].

For the present numerical analyzes we used sound-hard samples of 5 and 19 mm thickness, the latter corresponding to the experimental board (see Fig. 2.). The gap width w_G was varied between 0.3 and 2 mm. The results are presented in the following section.

5. Results and Discussion

Figure 5. displays the RMS velocity in the gap region of the *Thermoviscous Acoustics* domain. The depth of the slit is 5 mm, which corresponds to the thickness of the sound-hard board. The maximum loss factor $\beta = 1$ is obtained for a gap width of 0.5 mm and a frequency of 175 Hz of the incident wave. In this case the RMS velocity profile across the gap is almost parabolic, as can be inferred from Fig. 5. The property of a parabolic velocity profile is used below to generate a compact model of sound attenuation within the gap, see section 6. From the velocity values in figure 5. it can be deduced that a considerable volume of air outside the opening is agitated vigorously and is affected by the constriction. This fact is taken into account in an effective slit depth, see section 6.

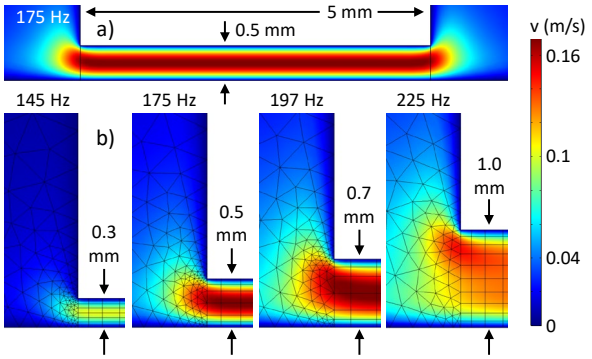

Figure 5. RMS velocity in the slit of the 5 mm board. Illustration **a)** at the top displays the velocity along the entire slit depth of 5 mm at 175 Hz. The gap is 0.5 mm wide. The diagram corresponds to the maximum loss factor $\beta = 1$. **b)** RMS velocities at the slit entrance for various gap widths. The frequency above each diagram corresponds to the maximum loss factor β for the indicated gap width. Note the smoothness of the velocities across the domain that justifies the choice of the mesh (see text).

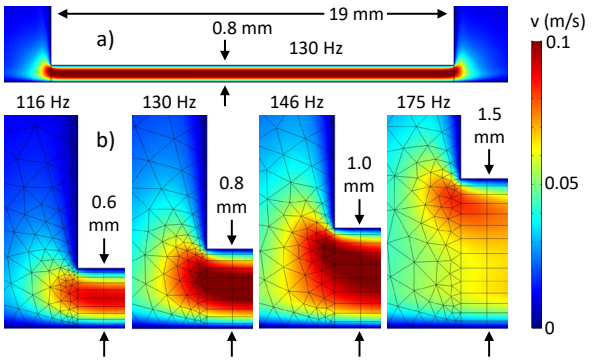

Figure 6. RMS velocity in the slit of the 19 mm plate. **a)** The picture presents the velocity along the entire slit depth of 19 mm at 130 Hz. The gap is 0.8 mm wide. The diagram corresponds to a loss factor of $\beta = 1$. **b)** RMS velocities at the slit entrance for various gap widths. The frequencies above each diagram belong to the maximum loss factor β for the specified gap widths.

Fig. 6. presents the same diagrams as in figure 5. Only that now the slit length is 19 mm, which corresponds to the thickness of the MDF-board used in the experiment. The maximum loss factor $\beta = 1$ is reached for a gap width of 0.8 mm at a frequency of 130 Hz. Again, the velocity profiles are parabolic and the range of agitated air is larger than the gap volume.

Figs. 7. and 8. show the loss factor $\beta = 1 - |r|^2$ of the 5 mm board and the 19 mm board as a function of frequency f of the incident wave. Four different approaches are displayed in the figures to determine the loss factor β. Results derived from the *Thermoviscous Acoustics* model are shown as circles. The circles with the largest β of each color (i.e. of the different gap

widths) belong to the diagrams in the figures 5. and 6. The lines in Figs. 7. and 8. are obtained from *Narrow Region* computations. The dashed lines are the result of our own model (see next section). The black squares of figure 8. represent the experimental values. Note that the experimental points fit exactly the calculations of the 0.6 mm wide gap. The board was actually prepared with a gap of 0.5 mm. The deviation stems from the inaccuracy when cutting the board to size. The consistency between the various curves and evaluation methods is excellent for the 19 mm thick plate (Fig. 8.). The agreement is somewhat less for the 5 mm plate, especially for larger gap widths. The latter is not surprising. The underlaying velocity profiles of the *Narrow Region* domain and of our compact model are only correct for the aspect ratios of long and narrow channels. The 5 mm deep slit with channel widths greater than 1 mm no longer seem to fulfill this condition.

6. Compact Model

The impedance tube with a sound-hard board and a tiny air gap is the perfect model of a microperforated slit-absorber for perpendicular sound incidence. The effectiveness of sound attenuation can be investigated experimentally (see section 2.) as well as numerically (sections 3. and 4.). To better understand the role of the design parameters of microperforated slits-absorber panels we have generated a simple model of the absorption loss coefficient β. The model is implemented in the spreadsheet program EXCEL ® and is explained in the following.

The interior impedance Z_i of the specimen in the impedance tube is composed of the sample impedance Z_S and the gap impedance Z_G. The gap impedance is a series resistance of flow resistance and inertia of the air in the slit volume. The flow resistance is due to the air drag between two parallel plates of small separation. The textbook expression (e.g. Ref. [9]) for this resistance is $R_G = \frac{\Delta p}{v_{av}} = 12\frac{\eta \cdot t_S}{w_G^2}$, where η is the dynamic viscosity of air, t_S is the slit depth (i.e. the sample thickness) and w_G is the width of the gap. This expression is based on a parabolic flow profile, which is confirmed in Figs. 5. and 6. The air contained inside the slit represents the inertia. The inertia contributes with the areal mass density $\varrho_A t_S$ to the impedance, where $\varrho_A \cong 1.2\ \frac{\mathrm{kg}}{\mathrm{m}^3}$ is the air density. The volume of air representing inertia is larger than the slit volume, see Figs. 5. and 6. Prof. Maa introduced a length end-correction factor of $\frac{4}{3}$ for circular holes in a microperforated plate, see Ref. [10]. For parallel plates instead of holes the value of the end correction is

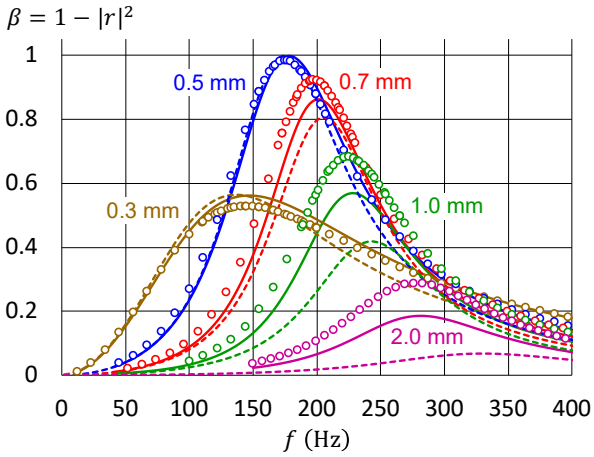

Figure 7. Loss factor of the 5 mm board versus frequency. The different colors represent different gap widths, indicated in the figure. The lines are the result of *Narrow Region* calculations. The circles stem from *Thermoviscous Acoustics* computations. The dashed lines are obtained by an EXCEL compact model (see section 6).

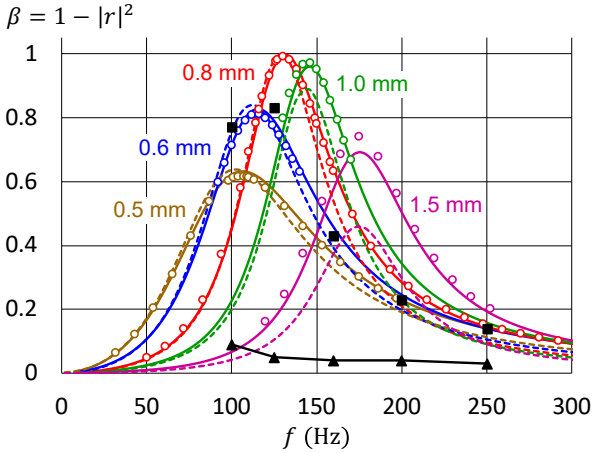

Figure 8. Loss factor of the 19 mm board versus frequency. The different colors are the different gap sizes. The numbers stand for the slit width. The circles, the lines and the dashed lines represent thermoviscous, *Narrow Region* and our own model calculations, respectively. Black symbols stand for experimental data. The black squares stem from measurements of the plate with slit (compare to Fig. 2.a). The triangles are the results of the plate with sealed gap (see Fig. 2.b). The black line guides the eye.

expected to be similar. Our end-correction employs the same factor plus an additive term, which was determined using figures 7. and 8. The areal mass density implemented in the spreadsheet model is $M_G = \varrho_A\left(\frac{4}{3}t_S + 2.7[\mathrm{mm}]\right)$. The slit impedance finally is:

$$Z_G = 12\frac{\eta \cdot t_S}{w_G^2} + i2\pi f \varrho_A\left(\frac{4}{3}t_S + 2.7[\mathrm{mm}]\right) \quad (3)$$

where i is the imaginary unit and f the frequency.

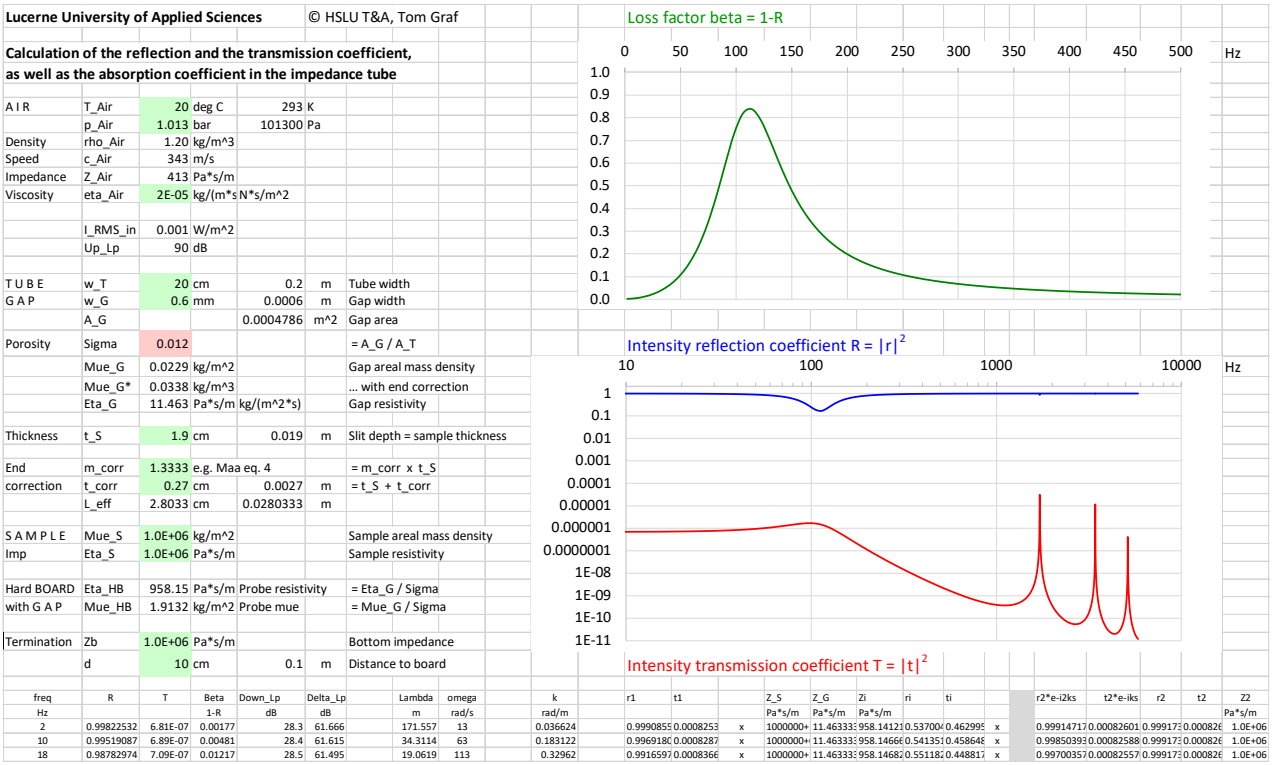

Figure 9. Excel spreadsheet that emulates the impedance tube calculations. The same layout can be used to compute the absorption of a microperforated slit-absorber. The green squares are input boxes, for example for the air temperature, for the absorber thickness, for the slit width, or for the distance of the sample panel to the bottom termination. The spreadsheet plots the loss factor β (upper graph) as well as the intensity reflection coefficient and the intensity transmission coefficient (lower graph). Note the different x-axes of the two graphs. The figure illustrates the calculation for a 19 mm thick panel with a 0.6 mm wide gap.

The total interior impedance is calculated as a parallel circuit with areal weighted impedances:

$$Z_i = \left(\frac{1}{Z_G \frac{A_T}{A_G}} + \frac{1}{Z_S \frac{A_T}{A_T - A_G}} \right)^{-1} = \left(\frac{\sigma}{Z_G} + \frac{(1-\sigma)}{Z_S} \right)^{-1} \quad (4)$$

where A_G is the gap area normal to the incident sound wave, A_T is the tube cross sectional area and $\sigma = \frac{A_G}{A_T}$ is the porosity. For example a stiff and air-tight board inserted in the tube and fastened to the supports exhibits a very large impedance Z_S, so that $Z_i = \frac{Z_G}{\sigma}$. The interior impedance Z_i is related to the pressure reflection coefficient $r_i = \frac{Z_i}{2Z_0 + Z_i}$ and the pressure transmission coefficient $t_i = 1 - r_i$, where $Z_0 = \varrho_A \cdot c \cong 410 \frac{\text{Pa·s}}{\text{m}}$ is the free space impedance of air. Utilizing the technique of transfer and scattering matrices Airy's equations for the total reflection and transmission coefficient can be derived, see e.g. Ref. [11]:

$$r = r_i + \frac{(t_i)^2 \, r_b \, e^{-i2kd}}{1 - r_i \, r_b \, e^{-i2kd}} \quad (5)$$

$$t = \frac{t_i \, t_b \, e^{-ikd}}{1 - r_i \, r_b \, e^{-i2kd}} \quad (6)$$

where r_b and t_b are the reflection and the transmission coefficient of the bottom termination cap of the impedance tube. d is the distance between the tube termination and the sample, see Fig. 3.

The equations (3) to (6) are implemented in EXCEL to plot the intensity loss factor $\beta = 1 - |r|^2$ as a function of frequency f, see figure 9. Input parameters are the gap width w_G, the sample thickness or slit depth t_S and the distance d of the simple to the termination cap. The input boxes are marked as green cases in Fig. 9. The porosity is calculated from geometry and is displayed in the pink case of the spreadsheet. Some EXCEL calculations are displayed in Figs. 7. and 8. as dashed lines. The comparison with COMSOL simulations und experiments is very good for gap widths smaller than 1.0 mm. For larger gaps the different curves diverge, but the frequency of the maximum loss factor β is still consistent.

7. Conclusions

The effect of an air gap around a sample in the impedance tube has been studied. A small air gap transforms a sound-hard sample plate into a slit-absorber displaying a characteristic absorption resonance. The experimental results can be reproduced precisely with FEM simulations, utilizing either thermoviscous models or so-called *Narrow Region* acoustics. The experimental and the numerical absorption curves can be emulated with a spreadsheet calculation model. The model is based on the simple idea of a parabolic velocity profile across the gap. For a specified low-frequency absorption band, the corresponding slit-plate-cavity dimensions can be found very quickly with the spreadsheet calculations. According to our model it is possible to achieve complete absorption for any frequency between 100 and 500 Hz, and even higher. By partitioning the panels into areas with different slits, porosities and adjacent air spaces, it should be possible to achieve broadband absorption. Using Maa's theory Herrin et al. suggest an alternative process to design optimal absorber panels [12].

The EN ISO 10534-2:2001 standard stipulates that the edge of the sample must be sealed. We are convinced that this is not enough to accurately determine the absorption of a material. The sample must in addition have an air-tight frame to prevent air from leaking into the gap.

8. References

1. Uno Ingard, "Notes on Sound Absorption Technology", ISBN 0-931784-28-X, Equation 4.5.10.
2. COMSOL Multiphysics ®, Version 5.4, http://www.comsol.com/
3. See COMSOL users guide and documentation: **About the Narrow Region Acoustics Models** and **Narrow Region Acoustics**
4. https://www.comsol.ch/blogs/theory-of-thermoviscous-acoustics-thermal-and-viscous-losses (last visited 25.7.2019)
5. https://www.comsol.ch/blogs/how-to-model-thermoviscous-acoustics-in-comsol-multiphysics (last visited 25.7.2019)
6. Michael Möser, Technische Akustik, 9. edition, Springer Vieweg, 2012,
wave-separation method: chapter 6.2.2, Eq. 6.28
minimum-maximum method: chapter 6.2.1
7. T. Graf and J. Pan, "Determination of the complex acoustic scattering matrix of a right-angled duct", J. Acoust. Soc. Am., **134**, 292-299 (2013)
8. Tutorial example in the COMSOL Application Library: "duct_right_angled_bend"
9. Bruce R. Munson, Donald F. Young, Theodore H. Okiishi, Wade W. Huebsch, "Fundamentals of Fluid Mechanics", sixth Ed., John Wiley & Sons, 2010
10. Dah-You Maa, "Microperforated-Panel Wideband Absorbers", Noise Control Engineering Journal, **29**, 77-84 (1987)
11. Bahaa E. A. Saleh and Malvin Carl Teich, "Fundamentals of Photonics", second edition, John Wiley & Sons, 2007, chapter 7.1, Airy's Formulas, Eq. 7.1-8
12. D. W. Herrin, X. Hua, and J. Liu, "Microperforated Panel Absorber Design: A Tutorial", 21st International Congress on Sound and Vibration (ICSV21), Beijing, China, 13-17 July 2014, https://www.researchgate.net/publication/280088717_Microperforated_panel_absorber_design_A_tutorial (last visited 13.8.2019)

9. Acknowledgements

The author would like to thank Dr. György Csikos for helpful discussions and for initiating the present study. This work was partially supported by Innosuisse.